Saudi Pharmaceutical Journal (2026) 34:35
https://doi.org/10.1007/s44446-026-00088-w

RESEARCH ARTICLE

TPC2 regulates proteomic remodeling, bioenergetic phenotypes, and mitochondrial stress adaptation in melanoma

Homood M. As Sobeai[1] · Ali Hanbashi[2] · Lama Binobaid[3] · Khalid Alhazzani[1] · Sarah M. Almufadhili[1] · Ahmed Altuwaijri[1] · Rashed Almousa[4] · Faroq Kamli[2] · Sulaiman S. Alhudaithi[5] · Moureq Alotaibi[1] · John Parrington[6]

Received: 4 February 2026 / Accepted: 14 April 2026

Abstract

Melanoma is a highly heterogeneous malignancy in which tumor behavior is shaped by complex signaling, trafficking, and metabolic programs. Two-pore channel 2 (TPC2), an endolysosomal ion channel, has been implicated in pigmentation, vesicular trafficking, and cancer-related cellular processes, but its role in melanoma remains incompletely understood. In this study, we investigated the impact of TPC2 loss in two melanoma models, the human cell line CHL-1 and the murine cell line B16, using previously validated CRISPR/Cas9-generated TPC2 knockout cells. Proteomic profiling, pathway enrichment analysis, extracellular flux measurements, and mitochondrial membrane potential assessment were used to define the molecular and functional consequences of TPC2 deletion. Proteomic analysis revealed marked but distinct changes in protein expression in CHL-1 and B16 cells, with clear separation between wild-type and TPC2 KO proteomic profiles in both models. Functional enrichment analysis showed that CHL-1 cells were preferentially associated with pathways related to metabolic regulation, morphogenesis, intracellular transport, extracellular matrix organization, and signaling networks including WNT and TGF-β, whereas B16 cells were enriched in immune/interferon-related pathways, protein homeostasis, intracellular trafficking, and stress-response programs. Bioenergetic profiling demonstrated that TPC2 KO altered cellular metabolism in a cell line-dependent manner. In CHL-1 cells, TPC2 loss reduced basal oxygen consumption rate (OCR) and the OCR/extracellular acidification rate (ECAR) ratio, but enhanced oxidative adaptation under glucose-free conditions. In contrast, B16 TPC2 KO cells displayed increased OCR and ECAR under basal conditions, consistent with a more energetically active phenotype. Despite these differences in basal bioenergetics, TPC2 KO preserved mitochondrial membrane potential under stress in both cell lines, indicating enhanced mitochondrial stress resilience. Collectively, these findings identify TPC2 as a context-dependent regulator of melanoma cell physiology that influences proteomic remodeling, metabolic adaptation, and mitochondrial function. These results support further investigation of TPC2 as a potential therapeutic target in melanoma, while emphasizing that its biological effects depend on cellular context.

Keywords TPC2 · Melanoma · CHL-1 · B16 · Proteomics · Bioenergetics · Mitochondrial membrane potential

✉ Homood M. As Sobeai
hassobeai@ksu.edu.sa

John Parrington
john.parrington@pharm.ox.ac.uk

[1] Department of Pharmacology and Toxicology, College of Pharmacy, King Saud University, P.O. Box 2457, 11451 Riyadh, Saudi Arabia

[2] Department of Pharmacology and Toxicology, College of Pharmacy, Jazan University, 45142 Jazan, Saudi Arabia

[3] Department of Pharmacology and Toxicology, College of Pharmacy, Umm Al-Qura University, 21955 Makkah, Saudi Arabia

[4] Department of Medical Equipment Technology, College of Applied Medical Sciences, Majmaah University, 11952 Majmaah, Saudi Arabia

[5] Department of Pharmaceutics, College of Pharmacy, King Saud University, P.O. Box 2457, 11451 Riyadh, Saudi Arabia

[6] Department of Pharmacology, University of Oxford, Mansfield Road, Oxford OX1 3QT, UK

Published online: 04 June 2026

1 Introduction

Melanoma is an aggressive malignancy of melanocytes characterized by marked molecular and phenotypic heterogeneity (Gray-Schopfer et al. 2007; Ng et al. 2022). Compared with many other solid tumors, melanoma exhibits a high tumor mutational burden and frequently harbors alterations in genes such as *BRAF*, *NRAS*, *NF1*, *PTEN*, *TP53*, and *CDKN2A* (Akbani et al. 2015; Moreira et al. 2021; Soura et al. 2016; Toussi et al. 2020). This heterogeneity contributes to substantial variability in tumor behavior, metastatic potential, therapeutic response, and metabolic adaptation (Beigi et al. 2024; Grzywa et al. 2017; Hachey and Boiko 2016). Accordingly, a deeper understanding of the molecular mechanisms that shape melanoma cell phenotypes remains essential for the development of more effective targeted therapies.

Among the emerging regulators of tumor cell behavior are the two-pore channels (TPCs), a family of endolysosomal ion channels involved in intracellular signaling and organelle homeostasis (Alharbi and Parrington 2019; Jin et al. 2024). TPC2, in particular, is localized predominantly to late endosomes and lysosomes, and has also been identified in melanosomes (Lagostena et al. 2025; Zhu et al. 2010). It has been implicated in the regulation of vesicular trafficking, ion homeostasis, pigmentation, autophagy-related pathways, and cellular signaling (Ambrosio et al. 2016; Grimm et al. 2017; Ogunbayo et al. 2018). Depending on context, TPC2 has been described as a channel regulated by NAADP-dependent Ca^{2+} signaling and by $PI(3,5)P_2$, placing it at the center of pathways linking endolysosomal function to broader cellular responses (Cang et al. 2014; Wang et al. 2012).

Accumulating evidence indicates that TPC2 plays an important role in cancer biology. Previous studies have shown that TPC2 contributes to processes relevant to tumor progression, including cell migration, invasion, neoangiogenesis, and adaptation to stress (Alharbi and Parrington 2019; Chen et al. 2022; Skelding et al. 2022). In melanoma, TPC2 has also been linked to melanosome biology and pigmentation (Zhu et al. 2010). Notably, pharmacological inhibition or genetic silencing of TPC2 in pigmented melanoma cells has been reported to increase melanin content while reducing proliferation, migration, and invasion(Ambrosio et al. 2015; Favia et al. 2014; Nguyen et al. 2017). However, the biological consequences of TPC2 disruption are not uniform across melanoma models (Abrahamian and Grimm 2021; Barbonari et al. 2024; Hanbashi et al. 2023; Netcharoensirisuk et al. 2021). This suggests that TPC2 may function not as a simple oncogenic or tumor-suppressive factor, but rather as a context-dependent regulator whose effects are shaped by the molecular and phenotypic background of the cell.

Our previous work supports this view. Using CRISPR/Cas9-edited melanoma models, we found that TPC2 loss produced divergent phenotypes in different melanoma cell lines. In the metastatic human melanoma cell line CHL-1, TPC2 knockout enhanced proliferative and invasive traits and was associated with altered expression of epithelial–mesenchymal transition–related markers, matrix remodeling proteins, and Hippo pathway components (Barbonari et al. 2024). In contrast, in B16 melanoma cells, TPC2 loss impaired invasive behavior (Barbonari et al. 2024). In vivo studies further showed that loss of TPC2 reduced tumor growth while increasing tumor-associated toxicity, underscoring the complexity of TPC2 function in melanoma (Hanbashi et al. 2023). Together, these observations suggest that TPC2 exerts multifaceted and model-dependent effects on melanoma progression.

Because proteins represent the major functional effectors of cellular phenotype, proteomic profiling offers a powerful strategy for defining the downstream consequences of TPC2 loss (Kwon et al. 2021; Shuken 2023). Proteomics can identify altered signaling networks, metabolic programs, trafficking pathways, and stress-response mechanisms that may not be evident from transcript-level analyses alone (Franks et al. 2017; Latonen et al. 2018; Mani et al. 2022; Ponomarenko et al. 2023). In melanoma, where phenotypic plasticity is a hallmark of disease progression, such an approach is particularly valuable for resolving how a single molecular perturbation can generate divergent biological outcomes in different cellular backgrounds (Huang et al. 2021; Rambow et al. 2019).

In addition to its roles in trafficking and signaling, TPC2 is well-positioned to influence cellular metabolism and mitochondrial function (de Zélicourt et al. 2024; Müller et al. 2021). Lysosomes and mitochondria communicate extensively to coordinate nutrient sensing, calcium homeostasis, autophagy, and metabolic adaptation (Deus et al. 2020; Giamogante et al. 2024; Nguyen et al. 2024; Tooze and Zoncu 2015). As an endolysosomal channel, TPC2 may therefore affect not only invasive and signaling phenotypes, but also the bioenergetic state of melanoma cells and their ability to adapt to metabolic stress (Abrahamian and Grimm 2021; Oluseye A. Ogunbayo et al. 2018; Skelding et al. 2022). Despite this possibility, the relationship between TPC2, melanoma cell metabolism, and mitochondrial function remains insufficiently characterized.

In the present study, we used previously validated TPC2 knockout CHL-1 and B16 melanoma cell lines to investigate how TPC2 loss alters melanoma cell physiology. We combined proteomic profiling, functional enrichment analysis, extracellular flux measurements, and mitochondrial membrane potential assessment to define the molecular and bioenergetic consequences of TPC2 deletion. Our findings show that TPC2 knockout induces broad but cell line–specific

proteomic remodeling, alters bioenergetic phenotypes in a context-dependent manner, and enhances the preservation of mitochondrial membrane potential under stress. These results identify TPC2 as a regulator of melanoma cell plasticity that links endolysosomal function to proteomic remodeling, metabolic adaptation, and mitochondrial stress resilience.

2 Materials and methods

2.1 Cell lines

The human melanoma cell line CHL-1 and the murine melanoma cell line B16 (ATCC, USA) were cultured in DMEM supplemented with with 2 mmol/L glutamine, 1 × penicillin/streptomycin (Sigma, USA) and 10% fetal bovine serum (FBS) (Gibco, USA). Cells were maintained under standard culture conditions at 37 °C in a humidified atmosphere containing 5% CO_2. The TPC2 KO models of both CHL-1 and B16 used in this study correspond to the same previously established and validated CRISPR/Cas9-edited clones described in our earlier work (D'Amore et al. 2020).

2.2 Protein quantification and mass spectrometry

Cells were lysed in NP-40 lysis buffer (50 mM Tris–HCl, pH 7.4, 150 mM NaCl, 1% NP-40) supplemented with protease inhibitors, incubated on ice for 30 min, and clarified by centrifugation at 12,000 × g for 10 min at 4 °C. Protein concentration was determined using the bicinchoninic acid (BCA) assay according to the manufacturer's instructions (Smith et al. 1985), and 40 µg of protein were used for downstream proteomic analysis.

For LC–MS/MS analysis, proteins were reduced with dithiothreitol (DTT) and alkylated with iodoacetamide (IAA) at room temperature for 30 min, followed by methanol/chloroform precipitation. Protein pellets were reconstituted in 400 mM Tris–HCl (pH 7.8) containing 6 M urea. After dilution of urea to 1 M, samples were digested overnight at 37 °C with trypsin at a 1:50 ratio. Digested peptides were acidified to a final concentration of 1% formic acid, desalted using Sola HRP SPE cartridges (Thermo Fisher Scientific, USA), and dried in a SpeedVac.

Peptides were analyzed using a Dionex Ultimate 3000 RSLC system coupled to an Orbitrap Fusion Lumos mass spectrometer (Thermo Fisher Scientific, USA). Online desalting was performed using a PepMAP C18 trap column, followed by peptide separation on an EASY-Spray PepMAP C18 analytical column over a 60-min gradient. MS scans were acquired over a range of 400–1,500 m/z at a resolution of 120,000, with an automatic gain control (AGC) target of 4.0×10^5. MS/MS spectra were collected in the linear ion trap in rapid scan mode after collision-induced dissociation at 35% collision energy, with an AGC target of 4.0×10^3 and a maximum injection time of 250 ms. The duty cycle was limited to 3 s, and precursor ions were dynamically excluded for 30 s to reduce repeated sampling (Davis et al. 2017).

2.3 Quantitative analysis of mass spectrometry data

Raw mass spectrometry data were processed using MaxQuant (version 1.6.2.3) (Cox and Mann 2008) with the MaxLFQ algorithm for label-free quantification (Cox et al. 2014). Database searches were performed against the curated UniProt Homo sapiens and Mus musculus reference proteomes, as appropriate. Trypsin specificity was applied with up to two missed cleavages allowed. Carbamidomethylation of cysteine was set as a fixed modification, whereas methionine oxidation and protein N-terminal acetylation were included as variable modifications. Peptide-spectrum match and protein false discovery rates (FDRs) were controlled at 1% using a reverse decoy strategy. The "match between runs" function was enabled.

The comparative quantitative analysis of protein abundance between WT and TPC2 KO samples was performed using Perseus (version 1.5.2.4). Label-free quantitation (LFQ) intensities from biological replicates were log-transformed and normalized by median subtraction. Proteins with insufficient data across replicates were excluded. Missing values were imputed based on a normal distribution. Principal component analysis, volcano plots, and hierarchical clustering were used to visualize proteomic differences between groups. Statistical significance was assessed using a Student's t-test with permutation-based FDR correction and 250 randomizations (Shuken 2023).

2.4 Functional enrichment and pathway analysis

To explore the biological significance of the differentially expressed proteins identified in TPC2 KO cells relative to WT cells, enrichment analysis was performed using WebGestalt (WEB-based Gene Set Analysis Toolkit; http://www.webgestalt.org/, 2017 revision). Gene Ontology (GO) enrichment was assessed across the categories Biological Process, Cellular Component, and Molecular Function. Pathway enrichment analysis was performed using the Reactome and Kyoto Encyclopedia of Genes and Genomes (KEGG) databases. Enriched terms and pathways were considered significant at an FDR threshold of 0.05 (Wang et al. 2013).

2.5 Measurement of cellular bioenergetics

Cellular bioenergetics were assessed using an XF96 Extracellular Flux Analyzer (Seahorse Bioscience, Billerica,

USA). Adherent cells were seeded into Seahorse XF96 Cell Culture Microplates at a density of 2×10^4 cells/well in complete growth medium and allowed to attach overnight at 37 °C. Plates were gently rocked at room temperature for 20–40 min after seeding to promote even cell distribution.

On the following day, growth medium was replaced with Seahorse phenol red-free DMEM containing either glucose or no glucose, depending on the experimental condition. Cellular respiration and acidification were then measured as oxygen consumption rate (OCR) and extracellular acidification rate (ECAR), respectively. OCR was used as an indicator of mitochondrial oxidative phosphorylation, whereas ECAR was used as an index of extracellular acidification associated with glycolytic and respiratory metabolism (Nadanaciva et al. 2012).

2.6 Measurement of mitochondrial membrane potential (MMP)

Mitochondrial membrane potential (MMP; $\Delta\Psi m$) was assessed using the JC-1 dye assay (Abcam, ab113850). Cells were seeded in 96-well plates at a density of 5×10^4 cells/well and incubated for 24 h. To induce stress, cells were then exposed to low-serum medium (0.5% FBS). After treatment, cells were washed with PBS and incubated with JC-1 dye diluted in PBS for 20 min at 37 °C in the dark. Cells were then washed and maintained in fresh PBS.

Fluorescence was measured using a Spark multimode microplate reader (Tecan) at excitation/emission wavelengths of 535/590 nm for red fluorescence (JC-1 aggregates) and 475/530 nm for green fluorescence (JC-1 monomers). After background subtraction, MMP was expressed as the red/green fluorescence ratio. For imaging experiments, red and green fluorescence channels were acquired sequentially to minimize spectral overlap (Sivandzade et al. 2019).

2.7 Statistical analysis

All experiments were performed using at least three independent biological replicates. Data are presented as mean ± SEM. Statistical comparisons between two groups were performed using an unpaired two-tailed Student's t-test with Welch's correction. For comparisons involving more than two groups, two-way analysis of variance (ANOVA) followed by Sidak's multiple-comparisons test was used. A p-value < 0.05 was considered statistically significant. Statistical analyses were performed using GraphPad Prism (version 6.0) and Microsoft Excel.

3 Results

3.1 TPC2 knockout induces distinct proteomic changes in CHL-1 and B16 melanoma cells

To investigate the molecular consequences of TPC2 loss in melanoma, we performed comparative proteomic profiling of TPC2 KO and WT cells in the human melanoma cell line CHL-1 and the murine melanoma cell line B16. Differential expression analysis comparing TPC2 KO with WT cells in CHL-1 revealed a discrete subset of significantly altered proteins, as visualized in a volcano plot (Fig. 1A). Unsupervised hierarchical clustering further demonstrated clear separation between WT and TPC2 KO samples, indicating that TPC2 deletion is associated with a reproducible shift in the CHL-1 proteomic profile (Fig. 1B).

The top differentially expressed proteins in CHL-1 cells are summarized in Fig. 1C and D. Among the most downregulated proteins in TPC2 KO cells were PPT1, ITGA6, and MAP1B, implicating pathways related to lysosomal function, cell adhesion, and cytoskeletal organization. In contrast, the most upregulated proteins included PCK1, HDAC1, RDH10, and ECE1, suggesting changes in metabolic regulation, chromatin-associated processes, and protein processing. Collectively, these data indicate that TPC2 loss in CHL-1 cells is associated with broad proteomic remodeling involving cellular architecture, trafficking, and metabolism.

In B16 cells, differential expression analysis showed a distinct set of proteins significantly altered by TPC2 knockout, as illustrated in the volcano plot (Fig. 1E). Hierarchical clustering showed clear segregation of WT and KO samples (Fig. 1F), supporting the robustness of the genotype-associated proteomic shift in this model, as observed in CHL-1.

The top differentially expressed proteins in B16 cells are shown in Figs. 1G and H. Among the most downregulated proteins in TPC2 KO cells were Serbp1, Hspa14, Trmt112, and Slc7a6, whereas the most upregulated proteins included Isg15, Fau, Ifitm3, Sumo2, and Sptan1. Notably, several of the upregulated proteins in B16 cells are linked to interferon-responsive and stress-associated pathways, suggesting that TPC2 loss in this model may engage immune- and stress-related signaling networks in addition to metabolic reprogramming. The full lists of differentially expressed proteins and their corresponding fold-change values in CHL-1 and B16 cells are provided in Supplementary Tables 1 and 2, respectively.

Overall, these findings demonstrate that TPC2 knockout produces significant, cell line–specific proteomic alterations in melanoma cells. While both CHL-1 and B16 cells showed clear separation between WT and KO proteomes, the identities of the most altered proteins differed substantially between the two models, supporting the context-dependent nature of the functional consequences of TPC2 loss.

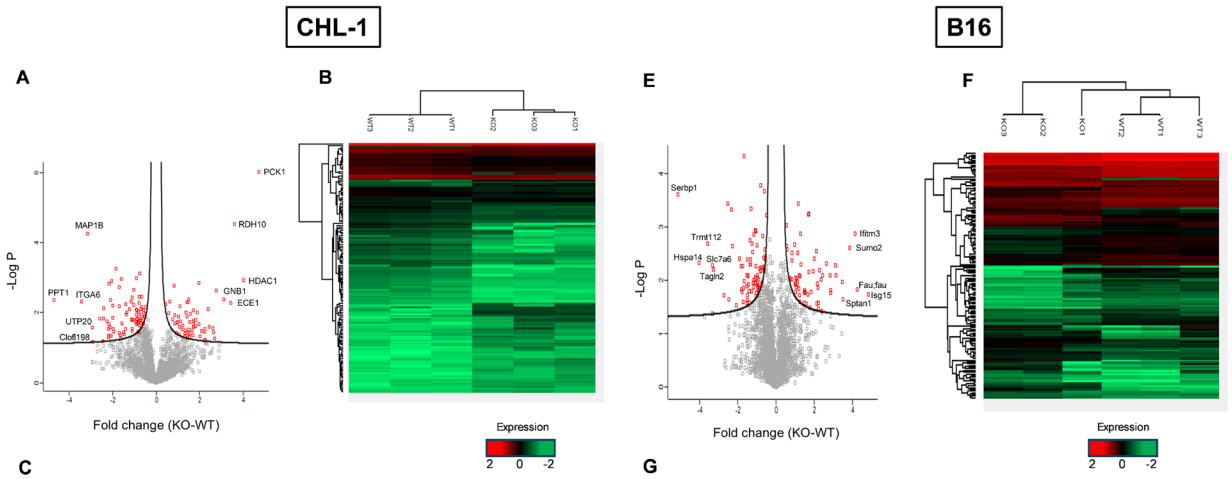

C

Top 15 downregulated proteins in CHL-1

#	Protein Symbol	Protein names	Fold Change (relative to WT)
1	PPT1	Palmitoyl-protein thioesterase 1	-4.68
2	ITGA6	Integrin alpha-6	-3.43
3	MAP1B	Microtubule-associated protein 1B	-3.14
4	UTP20	Small subunit processome component 20 homolog	-2.93
5	C1orf198	Uncharacterized protein C1orf198	-2.89
6	ARF5	ADP-ribosylation factor 5	-2.59
7	FST	Follistatin	-2.43
8	FSCN1	Fascin	-2.41
9	ZHX2	Zinc fingers and homeoboxes protein 2	-2.41
10	PRIM1	DNA primase small subunit	-2.26
11	CERS2	Ceramide synthase 2	-2.19
12	DCTPP1	dCTP pyrophosphatase 1	-2.18
13	SNX18	Sorting nexin-18	-2.18
14	DIAPH1	Protein diaphanous homolog 1	-2.17
15	KRAS	GTPase KRas;GTPase KRas, N-terminally processed	-2.17

G

Top 15 downregulated proteins in B16

#	Protein Symbol	Protein Name	Fold Change (relative to WT)
1	Serbp1	SERPINE1 MRNA Binding Protein 1	-5.15
2	Hspa14	Heat shock 70 kDa protein 14	-4.05
3	Trmt112	Multifunctional methyltransferase subunit TRM112	-3.58
4	Slc7a6	Y+L amino acid transporter 2	-3.34
5	Tagln2	Transgelin-2	-3.33
6	Pcbp2	Poly(rC)-binding protein 2	-3.29
7	Mlf2	Myeloid leukemia factor 2	-2.72
8	Cdc73	Parafibromin	-2.54
9	Tmed1	Transmembrane emp24 domain-containing protein 1	-2.48
10	Scd2	Acyl-CoA desaturase 2	-2.34
11	Leo1	RNA polymerase-associated protein LEO1	-2.29
12	Ints9	Integrator complex subunit 9	-2.10
13	Pih1d1	PIH1 domain-containing protein 1	-1.92
14	Agpat5	1-acyl-sn-glycerol-3-phosphate acyltransferase epsilon	-1.84
15	Exoc2	Exocyst complex component 2	-1.80

D

Top 15 upregulated proteins in CHL-1

#	Protein Symbol	Protein names	Fold Change (relative to WT)
1	PCK1	Phosphoenolpyruvate carboxykinase, cytosolic [GTP]	4.71
2	HDAC1	Histone deacetylase 1	4.01
3	RDH10	Retinol dehydrogenase 10	3.59
4	ECE1	Endothelin-converting enzyme 1	3.43
5	GNB1	Guanine nucleotide-binding protein, subunit beta-1	3.1
6	DDX18	ATP-dependent RNA helicase DDX18	2.76
7	SLC39A7	Zinc transporter SLC39A7	2.69
8	PODXL	Podocalyxin	2.64
9	ACTL8	Actin-like protein 8	2.61
10	IGFBP5	Insulin-like growth factor-binding protein 5	2.38
11	COX7A2	Cytochrome c oxidase subunit 7A2, mitochondrial	2.25
12	SNRPB2	U2 small nuclear ribonucleoprotein B	2.23
13	SMAD4	Mothers against decapentaplegic homolog 4	2.23
14	WDHD1	WD repeat and HMG-box DNA-binding protein 1	2.23
15	SEC14L2	SEC14-like protein 2	2.08

H

Top 15 upregulated proteins in B16

#	Protein Symbol	Protein names	Fold Change (relative to WT)
1	Isg15	Ubiquitin-like protein ISG15	4.84
2	Fau;fau	40S ribosomal protein S30	4.25
3	Ifitm3	Interferon-induced transmembrane protein 3	4.15
4	Sumo2	Small ubiquitin-related modifier 2	3.87
5	Sptan1	Alpha II-spectrin	3.51
6	Ddx58	Probable ATP-dependent RNA helicase DDX58	3.48
7	Lrba;Nbea	Lipopolysaccharide-responsive and beige-like anchor protein;Neurobeachin	3.15
8	Sntb2	Beta-2-syntrophin	3.1
9	Akr1c13	Aldo-keto reductase family 1 member C13	2.87
10	Lsm12	Protein LSM12 homolog	2.86
11	Acsl4	Long-chain-fatty-acid--CoA ligase 4	2.85
12	Gnpda1	Glucosamine-6-phosphate isomerase	2.63
13	Ptgr2	Prostaglandin reductase 2	2.45
14	Ap3s2	AP-3 complex subunit sigma-2	2.4
15	Tapbp	Tapasin	2.37

Fig. 1 Differential proteomic profiling of WT and TPC2 knockout melanoma cells. **A**) Volcano plot analysis of KO vs WT in CHL-1. Red points indicate proteins that were significantly altered. Gray points indicate proteins with no significant difference. **B**) A hierarchical cluster heat maps illustrate the connections between proteins (shown in rows) and different samples (shown in columns). The colors from green to red represent the relative protein levels between the two groups. **C**) the top 15 significantly downregulated proteins in TPC2 KO CHL-1 cells compared to WT CHL-1 cells. **D**) the top 15 significantly upregulated proteins in TPC2 KO CHL-1 cells relative to WT CHL-1 cells. **E**) Volcano plot of protein expression of KO vs WT B16 cells. Differentially expressed proteins are shown in red, while proteins with no significant difference are in gray. **F**) Hierarchical clustering of the differentially expressed proteins in the experimental samples of B16. **G**) the top 15 significantly downregulated proteins in TPC2 KO B16 cells compared to WT B16 cells. **H**) the top 15 significantly upregulated proteins in TPC2 KO B16 cells relative to WT B16 cells. Three independent biological replicates were used by each group. Statistical comparisons between WT and TPC2 KO cells were performed using an unpaired two-tailed t-test with Welch's correction. $P < 0.05$ is considered statistically significant

3.2 Functional enrichment analysis reveals distinct biological programs associated with TPC2 knockout in CHL-1 and B16 melanoma cells

Functional and pathway enrichment analyses were conducted using WebGestalt to identify potential functions and pathways enriched by differentially expressed proteins in CHL-1 KO cells relative to WT cells. Figure 2 illustrates GO biological Process and Reactome pathway enrichment, whereas Cellular Component, Molecular Function, and KEGG pathway results are presented in the supplementary Figs. 1 and 2.

In CHL-1 cells, GO biological process analysis identified enrichment of programs related to regulation of small-molecule metabolic processes, appendage development, morphogenesis of epithelium, response to oxygen levels, gland development, muscle cell differentiation, and carbohydrate homeostasis (Fig. 2A). Top negatively enriched processes were proteasomal protein catabolic process, organelle localization, ribonucleoprotein complex biogenesis, protein serine/threonine kinase signaling, regulation of actin filament-based processes, and intracellular transport.

Reactome analysis in CHL-1 cells further supported these observations by highlighting enrichment of pathways associated with GPCR signaling, signaling by nuclear receptors, WNT signaling, visual phototransduction, TGF-β receptor signaling, SMAD2/3:SMAD4 transcriptional regulation, and transport of small molecules (Fig. 2B). In addition, pathways linked to RNA metabolism and translation, extracellular matrix organization, cell–cell communication, ERBB2 signaling, lipid metabolism, and Rho GTPase signaling were negatively enriched. Together, these results indicate that TPC2 knockout in CHL-1 cells is associated with coordinated changes in signaling, transcriptional control, vesicular and small-molecule transport, extracellular matrix biology, and cytoskeletal dynamics.

In B16 cells, GO biological process analysis revealed a different enrichment profile, dominated by regulation of protein modification by small protein conjugation or removal, response to virus, proteasomal protein catabolic process, endosomal transport, protein homooligomerization, fatty acid metabolic process, intracellular receptor signaling, and positive regulation of secretion (Fig. 2C). negatively enriched processes included regulation of cellular protein localization, regulation of hematopoiesis, WNT-mediated cell–cell signaling, protein localization to the cytoskeleton, positive regulation of cell cycle, ncRNA metabolic process, and negative regulation of immune system processes. These data suggest that, in B16 cells, TPC2 loss preferentially affects protein turnover, immune- and virus-related

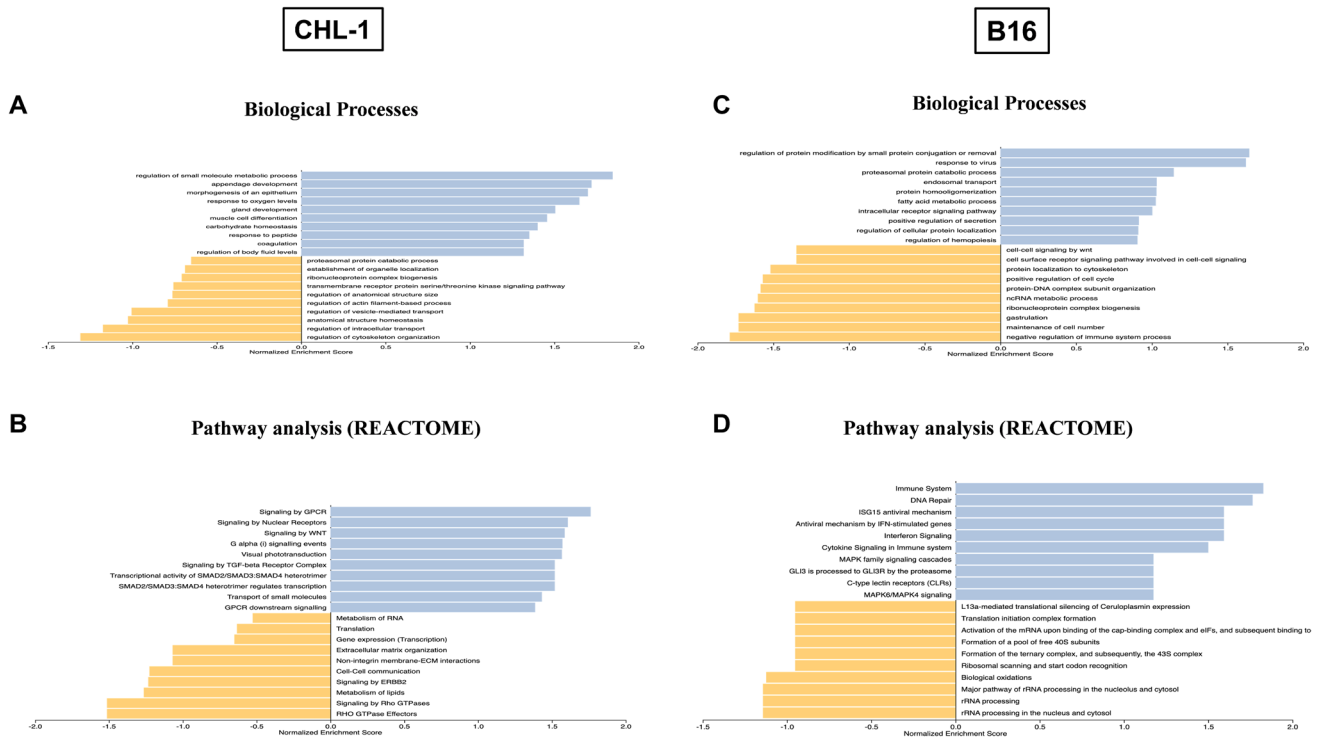

Fig. 2 Functional enrichment analysis of differentially expressed proteins in TPC2 knockout melanoma cells. Gene set enrichment analysis of proteins differentially expressed between WT and TPC2 KO melanoma cells was performed using WebGestalt. GO Biological Process enrichment in CHL-1 cells (**A**) and B16 (**C**). Reactome pathway enrichment in CHL-1 cells (**B**) and B16 (**D**). Enrichment analyses were performed using WebGestalt with an FDR threshold of 0.05

pathways, intracellular trafficking, lipid metabolism, and regulatory signaling networks.

Reactome analysis in B16 cells identified strong enrichment of Immune System, DNA Repair, ISG15 antiviral mechanism, antiviral mechanisms by IFN-stimulated genes, Interferon Signaling, Cytokine Signaling in Immune system, and MAPK family signaling cascades (Fig. 2D). Negative enrichment was observed in L13a-mediated translational silencing of ceruloplasmin expression, translation initiation, ribosomal scanning, and start codon recognition, biological oxidations, and rRNA processing. Overall, these results indicate that TPC2 knockout in B16 cells is strongly associated with immune/interferon-related programs, stress-response pathways, and RNA/translation-associated processes.

The supplementary analyses extended these findings. Cellular component and molecular function enrichment results are presented in Supplementary Fig. 1, while KEGG pathway enrichment is shown in Supplementary Fig. 2. In CHL-1 cells, KEGG analysis highlighted pathways in cancer, oxidative phosphorylation, viral carcinogenesis, and thyroid hormone signaling, along with enrichment for focal adhesion, regulation of the actin cytoskeleton, metabolic pathways, and endocytosis (Supplementary Fig. 2A). In B16 cells, KEGG analysis identified enrichment for RIG-I-like receptor signaling, autophagy, RNA transport, human cytomegalovirus infection, and several infection- and interferon-associated pathways, consistent with the immune- and stress-related pathways identified in the Reactome analysis (Supplementary Fig. 2B).

3.3 TPC2 knockout induces context-dependent bioenergetic reprogramming in melanoma cells

Proteomic analysis revealed enrichment in pathways related to mitochondrial function and cellular metabolism, including mitochondrial inner membrane organization, small-molecule metabolic processes, and mitochondrial protein complexes following TPC2 knockout. Given these findings, we next investigated whether TPC2 deletion alters cellular bioenergetics.

Cellular metabolism was assessed using a Seahorse XF96 extracellular flux analyzer by measuring oxygen consumption rate (OCR), an indicator of mitochondrial oxidative phosphorylation (OXPHOS), and extracellular acidification rate (ECAR), a surrogate marker of glycolytic activity. Under normal culture conditions, TPC2 knockout in CHL-1 cells resulted in a significant reduction in OCR (Fig. 3A-i), while ECAR remained largely unchanged (Fig. 3A-ii). Consequently, the OCR/ECAR ratio was decreased in KO cells compared with WT controls (Fig. 3A-iii), indicating a relative shift away from mitochondrial oxidative metabolism. These findings suggest that, under basal conditions, TPC2 deficiency in CHL-1 cells is associated with reduced mitochondrial respiratory activity without a compensatory increase in glycolysis, reflecting an overall altered metabolic state rather than a classical glycolytic switch.

To further probe metabolic flexibility, cells were cultured in glucose-free medium. Under these conditions, TPC2 KO cells exhibited a marked increase in OCR (Fig. 3B-i), along with an elevation in ECAR (Fig. 3B-ii). Notably, the OCR/ECAR ratio increased in KO cells, indicating a shift toward enhanced reliance on oxidative phosphorylation under metabolic stress (Fig. 3B-iii). Together, these results suggest that CHL-1 TPC2 KO cells display context-dependent metabolic reprogramming: impaired mitochondrial respiration under basal conditions but enhanced oxidative metabolism when glucose availability is limited.

In contrast to CHL-1 cells, TPC2 knockout in B16 cells induced a robust increase in both OCR and ECAR under normal culture conditions relative to WT cells (Fig. 3C-i, ii). This was accompanied by an elevated OCR/ECAR ratio (Fig. 3C-iii), indicating that KO cells adopt a more energetically active phenotype with a relative preference for oxidative metabolism.

Under glucose-free conditions, both WT and KO cells exhibited increased OCR, consistent with a compensatory shift toward mitochondrial respiration in the absence of glycolytic substrates (Fig. 4D-i). ECAR also increased modestly in both groups (Fig. 4D-ii), likely reflecting contributions from mitochondrial CO_2 production rather than glycolysis alone. Importantly, no significant difference in OCR/ECAR ratio was observed between WT and KO cells under glucose deprivation (Fig. 4D-iii), suggesting that while TPC2 KO enhances overall metabolic activity, it does not markedly alter the relative balance between oxidative and glycolytic pathways under these conditions.

3.4 TPC2 knockout preserves mitochondrial membrane potential under stress

To determine whether the bioenergetic changes associated with TPC2 knockout were accompanied by alterations in mitochondrial function, mitochondrial membrane potential (MMP; $\Delta\Psi m$) was assessed using the JC-1 probe. In this assay, red JC-1 aggregates indicate polarized mitochondria, whereas green JC-1 monomers indicate mitochondrial depolarization. Accordingly, the red/green fluorescence ratio was used as a quantitative index of MMP. Under basal conditions, the representative fluorescence images showed broadly similar red and green staining patterns between WT and TPC2 KO cells in both melanoma models (Fig. 4Ai, Ci), indicating no obvious genotype-dependent difference in mitochondrial polarization. Consistent with these images, quantification of the red/green JC-1 ratio showed no significant difference between WT and KO cells under basal conditions (Fig. 4Aii, Cii).

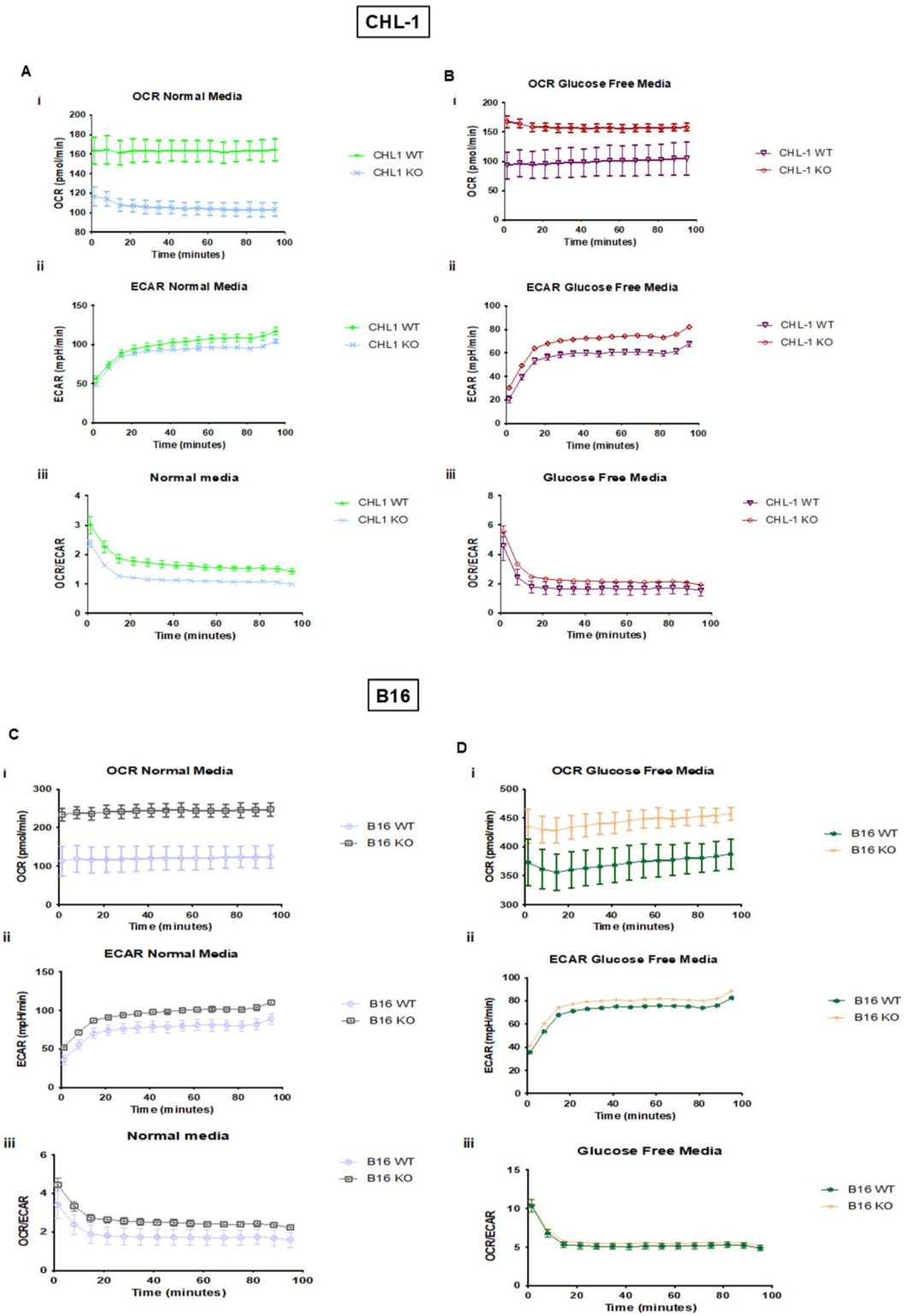

Fig. 3 Impact of TPC2 knockout on metabolic phenotypes of Melanoma cells. (**A**–**B**) CHL-1 cells and (**C**–**D**) B16 cells were analyzed under normal and glucose-free conditions, respectively. (i) Oxygen consumption rate (OCR), (ii) extracellular acidification rate (ECAR), and (iii) OCR/ECAR ratio were measured over time using a Seahorse XF96 extracellular flux analyzer. Under normal conditions, TPC2 knockout reduced OCR and the OCR/ECAR ratio in CHL-1 cells, whereas in B16 cells, it increased both OCR and ECAR, resulting in a higher OCR/ECAR ratio. Under glucose-free conditions, both cell lines exhibited increased OCR, consistent with enhanced reliance on oxidative phosphorylation. Data are presented as mean ± SEM from three independent biological replicates, each measured in technical triplicates. Statistical comparisons between WT and TPC2 KO cells were performed using two-way ANOVA followed by Sidak's multiple-comparisons test. $P < 0.05$ is considered statistically significant

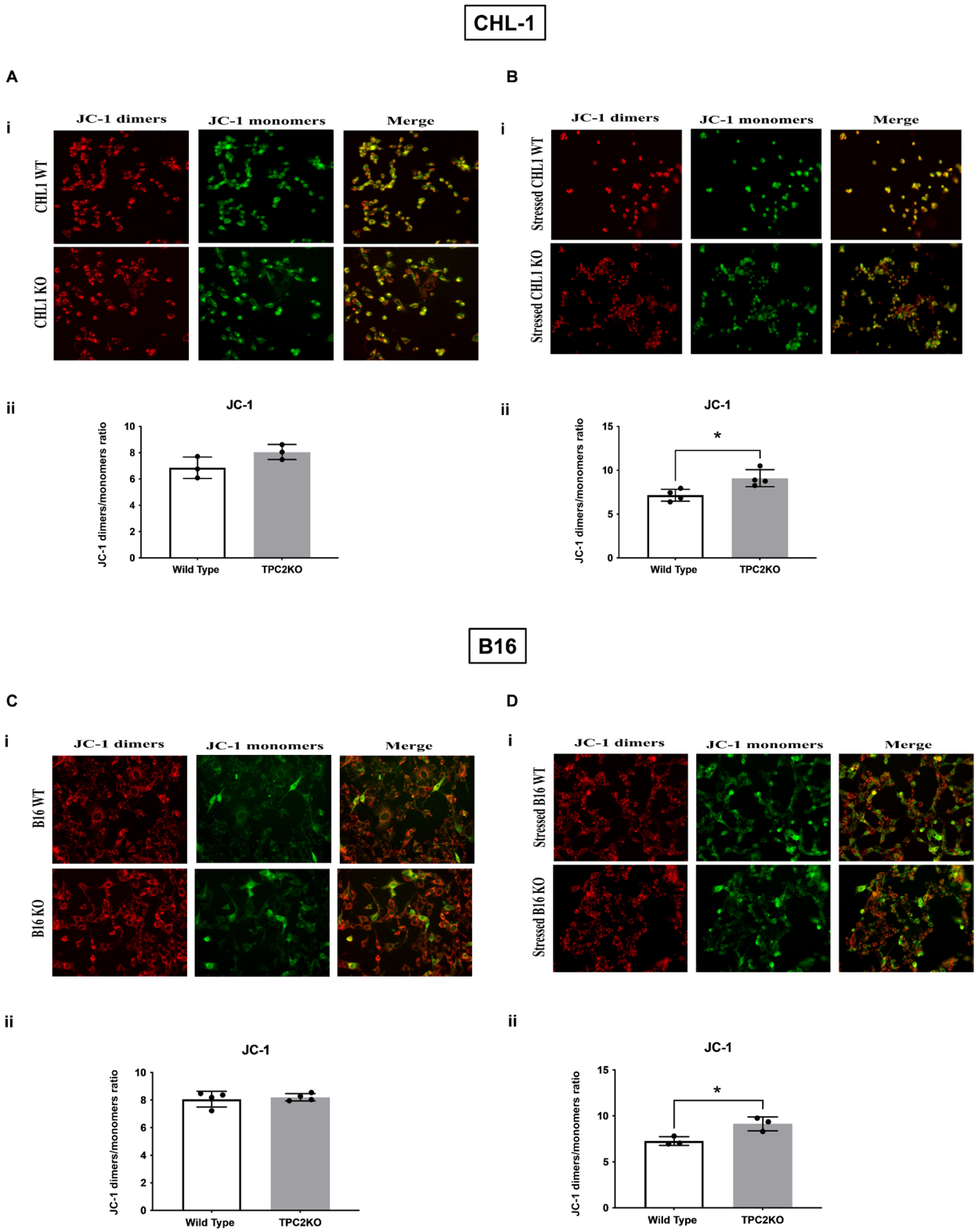

Fig. 4 Impact of TPC2 knockout on Mitochondrial membrane potential. Representative JC-1 fluorescence images of CHL-1 (**A**, **B**) and B16 (**C**, **D**) cells under basal (**A**, **C**) and stress conditions (0.5% FBS; **B**, **D**). Red fluorescence (aggregates) indicates polarized mitochondria, while green fluorescence (monomers) reflects depolarization. TPC2 knockout does not substantially alter mitochondrial membrane potential under basal conditions but significantly preserves mitochondrial polarization under stress in both CHL-1 and B16 melanoma cells. Quantification (Aii–Dii) is presented as the red/green fluorescence ratio. Results are expressed as the mean ± SD from at least three independent experiments. Statistical significance was assessed using an unpaired two-tailed t-test with Welch's correction. $P < 0.05$ is considered significant. Scale bar: 20 µm

In contrast, under stress conditions induced by serum deprivation, the representative microscopy images showed a clear difference between genotypes in both cell lines (Fig. 4Bi, Di). In CHL-1 cells, stressed WT cells exhibited relatively stronger green fluorescence, consistent with mitochondrial depolarization, whereas TPC2 KO cells retained more red fluorescence, indicating preservation of mitochondrial polarization (Fig. 4Bi). The corresponding quantitative analysis confirmed this pattern, with a significant increase in the red/green JC-1 ratio in TPC2 KO cells compared with the WT cells (Fig. 4Bii). A similar trend was observed in B16 cells, where stressed WT cells displayed a more prominent green signal, while TPC2 KO cells maintained stronger red fluorescence (Fig. 4Di). Quantification supported the microscopy findings, showing a statistically significant increase in the red/green ratio in TPC2 KO cells under stress relative to WT cells (Fig. 4Dii). Collectively, both the representative JC-1 images and the quantified red/green fluorescence ratios indicate that TPC2 knockout does not substantially alter mitochondrial membrane potential under basal conditions but significantly preserves mitochondrial polarization under stress in both CHL-1 and B16 melanoma cells.

4 Discussion

This study provides an integrated proteomic and functional analysis of the role of TPC2 in melanoma biology using two distinct models, the human cell line CHL-1 and the murine cell line B16. TPC2 has been knocked out using the CRISPR Cas9 system. The impaired protein expression has been validated in previous work (D'Amore et al. 2020). The current study shows that loss of TPC2 produces broad but context-dependent effects on melanoma cells. Although TPC2 knockout altered key pathways in both models, the direction and biological consequences of these changes differed between CHL-1 and B16 cells. These findings reinforce the idea that TPC2 is not a unidirectional regulator of melanoma behavior, but rather a multifunctional determinant of tumor cell physiology whose effects depend on cellular context.

The proteomic analysis demonstrated that TPC2 knockout induces substantial remodeling of the melanoma proteome in both cell lines. Interestingly, differentially expressed proteins are distinct between CHL-1 and B16 cells, suggesting that the downstream consequences of TPC2 deletion may be cell line-specific. This observation is consistent with previous reports showing that TPC2 can exert divergent effects depending on melanoma subtype, differentiation state, or metastatic potential (D'Amore et al. 2020; Hanbashi et al. 2023). In this regard, our findings extend earlier work by showing that these phenotypic differences are accompanied by distinct proteomic signatures, thereby providing a broader molecular framework for understanding how TPC2 contributes to melanoma heterogeneity.

The enrichment analyses further emphasized this context dependence. In CHL-1 cells, TPC2 knockout preferentially affected pathways related to metabolic regulation, morphogenesis, intracellular transport, extracellular matrix organization, and cytoskeletal dynamics, together with signaling networks such as WNT and TGF-β. These patterns are consistent with our earlier observations that TPC2 loss in CHL-1 cells promotes a more invasive phenotype and modifies Hippo-related signaling (D'Amore et al. 2020). In contrast, B16 cells displayed enrichment profiles dominated by immune/interferon-related pathways, protein homeostasis, intracellular trafficking, endosomal transport, and stress-associated programs. This divergence suggests that TPC2 loss may engage fundamentally different adaptive networks in the two melanoma models. Thus, while TPC2 appears to regulate broad cellular homeostasis in both systems, the specific biological programs that emerge following its deletion may be shaped by the intrinsic state of the cell.

A major finding of the present study is that TPC2 also influences melanoma cell bioenergetics. Proteomic enrichment of mitochondrial- and metabolism-associated categories urged us to evaluate the functional metabolic consequences of TPC2 loss. The extracellular flux data showed that the effect of TPC2 knockout on cellular bioenergetics is again highly context dependent. In CHL-1 cells, TPC2 knockout reduced OCR under basal conditions and lowered the OCR/ECAR ratio, indicating reduced mitochondrial respiratory activity relative to extracellular acidification. Notably, this was not accompanied by a major increase in ECAR, suggesting that TPC2 loss in CHL-1 cells does not simply induce a classical shift toward glycolysis, but rather alters the overall balance of energy metabolism. However, when glucose was removed from the medium, CHL-1 TPC2 KO cells increased OCR and displayed a higher OCR/ECAR ratio, indicating greater reliance on oxidative metabolism under nutrient stress. The enhanced oxidative adaptation of CHL-1 TPC2 KO cells under glucose deprivation is in line with previous work showing that TPC2 deficiency can alter cancer-cell energy metabolism and favor oxidative metabolism under glucose-free conditions (Müller et al. 2021). This pattern suggests that TPC2-deficient CHL-1 cells retain considerable metabolic flexibility and can adapt to glucose limitation by engaging mitochondrial respiration more strongly.

In B16 cells, the bioenergetic phenotype was different. TPC2 knockout increased both OCR and ECAR under normal culture conditions, with a net increase in OCR/ECAR ratio, consistent with a more energetically active phenotype showing relative preference for oxidative metabolism. Under glucose-free conditions, OCR increased in both WT and KO cells, as expected when cells are forced to rely less on

glycolytic substrate availability, but the OCR/ECAR ratio was not markedly different between genotypes. These results indicate that in B16 cells, TPC2 loss primarily promotes a globally elevated bioenergetic state rather than a simple directional switch between glycolysis and oxidative phosphorylation. Taken together, the Seahorse data indicate that TPC2 modulates metabolic plasticity, but that the specific consequences of its loss differ between melanoma models (Al-Masri et al. 2021; Hönigova et al. 2022).

The mitochondrial membrane potential results provide important additional context for interpreting the bioenergetic data. Under basal conditions, no major genotype-dependent differences in MMP were detected in either CHL-1 or B16 cells. Under serum-deprivation stress, however, TPC2 KO cells in both models preserved mitochondrial polarization more effectively than WT cells. These findings do not imply that TPC2 loss universally increases mitochondrial function at baseline. Rather, they suggest that TPC2 deficiency enhances the ability of melanoma cells to maintain mitochondrial integrity under stress, potentially through altered lysosomal signaling and mitochondria–lysosome crosstalk (Deus et al. 2020; Ogunbayo et al. 2018). This interpretation is consistent with the extracellular flux data, where mitochondria adapted to the metabolic challenge in both models.

The link between the enrichment analyses and the mitochondrial findings is biologically plausible. TPC2 is a lysosomal/endolysosomal ion channel with established roles in ion homeostasis, vesicular trafficking, organelle communication, and calcium signaling (Deus et al. 2020; Grossmann et al. 2021; Yuan et al. 2022; Zhu et al. 2010). These processes are closely connected to mitochondrial regulation. Mitochondria and lysosome-related organelles engage in extensive bidirectional signaling that influences nutrient sensing, autophagy, ROS handling, calcium flux, and metabolic adaptation (Deus et al. 2020; Nguyen et al. 2024; Park et al. 2022; Zhang et al. 2016). Alterations in pathways related to intracellular trafficking, organelle localization, endosomal transport, and metabolism; therefore, provide a reasonable molecular framework for the functional phenotypes we observed. Importantly, the enrichment analyses do not prove enhanced mitochondrial adaptation; rather, they provide a mechanistic context for the functional evidence from Seahorse and JC-1 assays. In this sense, the proteomic and functional data are complementary: the former identifies the pathways potentially perturbed by TPC2 loss, while the latter demonstrates their physiological consequences.

The relationship between TPC2 and mTOR- and calcium-dependent signaling may be particularly relevant in this context. Previous studies have shown that TPC2 is functionally linked to lysosomal nutrient sensing and to mTOR-dependent regulation of cellular metabolic state (Cang et al. 2013; Chang et al. 2020). TPC2 has also been implicated in NAADP-dependent and PI(3,5)P2-dependent signaling (Yuan et al. 2022), further supporting a role in integrating environmental cues with organellar responses. In addition, prior work has connected TPC2 to melanoma cell migration, invasion, and melanin synthesis (Ambrosio et al. 2016; Netcharoensirisuk et al. 2021; Nguyen et al. 2017), while other studies have demonstrated crosstalk between calcium signaling and pro-tumorigenic pathways such as Hippo/YAP/TAZ (Cunningham and Hansen 2022; Fu et al. 2022; Zhu et al. 2023). Our findings are compatible with a model in which TPC2 loss modifies lysosomal signaling and organelle cross-talk, thereby reshaping both the proteomic landscape and the metabolic behavior of melanoma cells. Whether the bioenergetic and mitochondrial phenotypes observed here are mediated directly through altered lysosomal calcium release, mTOR signaling, autophagic flux, or other pathways remains to be determined experimentally.

Although this study is strengthened by the use of two biologically distinct melanoma models and by integrating proteomic and functional analyses, several limitations should be acknowledged. First, this study relies on only two cell lines, which cannot fully represent the biological heterogeneity of melanoma, especially given the divergent phenotypic responses observed between CHL-1 and B16 cells, suggesting that therapeutic targeting of TPC2 may produce context-dependent, potentially unintended consequences. Second, although the enrichment analyses provide strong pathway-level clues, they do not establish direct causal links between specific proteins and the observed functional phenotypes. Third, OCR/ECAR measurements provide an informative overview of metabolic state, but ECAR should be interpreted cautiously because extracellular acidification can reflect both glycolysis-derived proton release and mitochondrial CO2 hydration (Mookerjee et al. 2015; Schmidt et al. 2021). Finally, JC-1 measurements indicate preservation of membrane potential under stress, but, by themselves, do not define the precise mechanisms responsible for this effect. Future work should therefore extend these findings to additional melanoma models, particularly in cell lines showing similar phenotypic consequences of TPC2 loss, incorporate in vivo validation, and directly test the involvement of candidate pathways such as mTOR, lysosomal calcium signaling, autophagy, and Hippo/YAP/TAZ signaling.

5 Conclusions

Our study demonstrates that TPC2 knockout induces marked but context-dependent effects in melanoma cells. In both CHL-1 and B16 models, loss of TPC2 produced distinct proteomic changes and pathway enrichment profiles, indicating broad remodeling of cellular programs. Functionally, TPC2 deletion altered bioenergetic

phenotypes in a cell line–specific manner, while consistently preserving mitochondrial membrane potential under stress in both models. Together, these findings identify TPC2 as a regulator of melanoma cell plasticity, metabolic adaptation, and mitochondrial stress resilience. These results support further investigation of TPC2 as a potential therapeutic target in melanoma, while underscoring that its biological effects are highly context-dependent.

Supplementary Information The online version contains supplementary material available at https://doi.org/10.1007/s44446-026-00088-w.

Acknowledgements The authors have reviewed and edited the output and take full responsibility for the content of this publication.

Author contributions Conceptualization, H.M.A.S., A.H and J.P.; methodology, H.M.A., A.H., L.B., K.A., S.A., A.A., R.A., F.K., S.S.A and M.A.; validation, H.M.A., A.H., L.B., K.A., S.A., A.A., R.A., F.K. and M.A.; formal analysis, H.M.A., A.H., L.B., K.A., S.A., A.A., R.A., F.K., M.A. and J.P.; investigation, H.M.A., A.H., L.B., K.A., S.A., A.A., R.A., F.K., S.S.A and M.A.; resources, H.M.A.S., A.H. and J.P.; data curation, H.M.A., A.H., L.B., K.A., S.A., A.A., R.A., F.K., S.S.A and M.A.; writing—original draft preparation, H.M.A., A.H., L.B., K.A., S.A., A.A., R.A., F.K., S.S.A., M.A. and J.P.; writing—review and editing, H.M.A., A.H., L.B., K.A., S.A., A.A., R.A., F.K., S.S.A, M.A. and J.P.; visualization, H.M.A.S, A.H., F.K.; supervision, J.P.; project administration, H.M.A.S, A.H. and J.P.; funding acquisition, H.M.A.S. All authors have read and agreed to the published version of the manuscript.

Funding This work was funded by Ongoing Research Funding Program number (ORF-2026–1478), King Saud University, Riyadh, Saudi Arabia.

Data availability Data sets generated in this study are available on reasonable request to the corresponding author.

Declarations

Institutional review board statement Not applicable.

Informed consent Not applicable.

Conflicts of interest The authors declare no conflicts of interest.

References

Abrahamian, C., Grimm, C., 2021. Endolysosomal Cation Channels and MITF in Melanocytes and Melanoma. Biomolecules 11. https://doi.org/10.3390/biom11071021

Akbani R, Akdemir KC, Aksoy BA, Albert M, Ally A, Amin SB, Arachchi H, Arora A, Auman JT, Ayala B, Baboud J, Balasundaram M, Balu S, Barnabas N, Bartlett J, Bartlett P, Bastian BC, Baylin SB, Behera M, …, Zou L (2015) Genomic Classification of Cutaneous Melanoma. Cell 161:1681–1696. https://doi.org/10.1016/j.cell.2015.05.044

Al-Masri M, Paliotti K, Tran R, Halaoui R, Lelarge V, Chatterjee S, Wang L-T, Moraes C, McCaffrey L (2021) Architectural control of metabolic plasticity in epithelial cancer cells. Commun Biol 4:371. https://doi.org/10.1038/s42003-021-01899-4

Alharbi AF, Parrington J (2019) Endolysosomal Ca2+ Signaling in Cancer: The Role of TPC2, From Tumorigenesis to Metastasis. Front Cell Dev Biol 7. https://doi.org/10.3389/fcell.2019.00302

Ambrosio AL, Boyle JA, Aradi AE, Christian KA, Di Pietro SM (2016) TPC2 controls pigmentation by regulating melanosome pH and size. Proc Natl Acad Sci U S A 113:5622–5627. https://doi.org/10.1073/pnas.1600108113

Ambrosio AL, Boyle JA, Di Pietro SM (2015) TPC2 mediates new mechanisms of platelet dense granule membrane dynamics through regulation of Ca^{2+} release. Mol Biol Cell 26:3263–3274. https://doi.org/10.1091/mbc.e15-01-0058

Barbonari S, D'Amore A, Hanbashi AA, Palombi F, Riccioli A, Parrington J, Filippini A (2024) Endolysosomal two-pore channel 2 plays opposing roles in primary and metastatic malignant melanoma cells. Cell Biol Int 48:521–540. https://doi.org/10.1002/cbin.12129

Beigi YZ, Lanjanian H, Fayazi R, Salimi M, Hoseyni BHM, Noroozizadeh MH, Masoudi-Nejad A (2024) Heterogeneity and molecular landscape of melanoma: implications for targeted therapy. Mol Biomed 5:17. https://doi.org/10.1186/s43556-024-00182-2

Cang C, Bekele B, Ren D (2014) The voltage-gated sodium channel TPC1 confers endolysosomal excitability. Nat Chem Biol 10:463–469. https://doi.org/10.1038/nchembio.1522

Cang C, Zhou Y, Navarro B, Seo Y, Aranda K, Shi L, Battaglia-Hsu S, Nissim I, Clapham DE, Ren D (2013) mTOR regulates lysosomal ATP-sensitive two-pore Na+ channels to adapt to metabolic state. Cell 152:778–790. https://doi.org/10.1016/j.cell.2013.01.023

Chang F-S, Wang Y, Dmitriev P, Gross J, Galione A, Pears C (2020) A two-pore channel protein required for regulating mTORC1 activity on starvation. BMC Biol 18:8. https://doi.org/10.1186/s12915-019-0735-4

Chen C-C, Krogsaeter E, Kuo C-Y, Huang M-C, Chang S-Y, Biel M (2022) Endolysosomal cation channels point the way towards precision medicine of cancer and infectious diseases. Biomed Pharmacother 148:112751. https://doi.org/10.1016/j.biopha.2022.112751

Cox J, Hein MY, Luber CA, Paron I, Nagaraj N, Mann M (2014) Accurate proteome-wide label-free quantification by delayed normalization and maximal peptide ratio extraction, termed MaxLFQ. Mol Cell Proteomics 13:2513–2526. https://doi.org/10.1074/mcp.M113.031591

Cox J, Mann M (2008) MaxQuant enables high peptide identification rates, individualized p.p.b.-range mass accuracies and proteome-wide protein quantification. Nat Biotechnol 26:1367–1372. https://doi.org/10.1038/nbt.1511

Cunningham R, Hansen CG (2022) The hippo pathway in cancer: YAP/TAZ and TEAD as therapeutic targets in cancer. Clin Sci (Lond) 136:197–222. https://doi.org/10.1042/CS20201474

D'Amore A, Hanbashi AA, Di Agostino S, Palombi F, Sacconi A, Voruganti A, Taggi M, Canipari R, Blandino G, Parrington J, Filippini A (2020) Loss of Two-Pore Channel 2 (TPC2) Expression Increases the Metastatic Traits of Melanoma Cells by a Mechanism Involving the Hippo Signalling Pathway and Store-Operated Calcium Entry. Cancers (Basel) 12:2391. https://doi.org/10.3390/cancers12092391

Davis S, Charles PD, He L, Mowlds P, Kessler BM, Fischer R (2017) Expanding proteome coverage with CHarge ordered parallel ion aNalysis (CHOPIN) combined with broad specificity proteolysis. J Proteome Res 16:1288–1299. https://doi.org/10.1021/acs.jproteome.6b00915

de Zélicourt A, Fayssoil A, Mansart A, Zarrouki F, Karoui A, Piquereau J, Lefebvre F, Gerbaud P, Mika D, Dakouane-Giudicelli M, Lanchec E, Feng M, Leblais V, Bobe R, Launay J-M, Galione A, Gomez AM, de la Porte S, Cancela J-M (2024) Two-pore channels (TPCs) acts as a hub for excitation-contraction coupling, metabolism and cardiac hypertrophy signalling. Cell Calcium 117:102839. https://doi.org/10.1016/j.ceca.2023.102839

Deus CM, Yambire KF, Oliveira PJ, Raimundo N (2020) Mitochondria-Lysosome Crosstalk: From Physiology to Neurodegeneration. Trends Mol Med 26:71–88. https://doi.org/10.1016/j.molmed.2019.10.009

Favia A., Desideri M, Gambara G, D'Alessio A, Ruas M, Esposito B, Del Bufalo D, Parrington J, Ziparo E, Palombi F, Galione A, Filippini A (2014) VEGF-induced neoangiogenesis is mediated by NAADP and two-pore channel-2–dependent Ca^{2+} signaling. Proc Natl Acad Sci 111. https://doi.org/10.1073/pnas.1406029111

Franks A, Airoldi E, Slavov N (2017) Post-transcriptional regulation across human tissues. PLoS Comput Biol 13:e1005535. https://doi.org/10.1371/journal.pcbi.1005535

Fu M, Hu Y, Lan T, Guan K-L, Luo T, Luo M (2022) The Hippo signalling pathway and its implications in human health and diseases. Signal Transduct Target Ther 7:376. https://doi.org/10.1038/s41392-022-01191-9

Giamogante F, Barazzuol L, Maiorca F, Poggio E, Esposito A, Masato A, Napolitano G, Vagnoni A, Calì T, Brini M (2024) A SPLICS reporter reveals α-synuclein regulation of lysosome-mitochondria contacts which affects TFEB nuclear translocation. Nat Commun 15:1516. https://doi.org/10.1038/s41467-024-46007-2

Gray-Schopfer V, Wellbrock C, Marais R (2007) Melanoma biology and new targeted therapy. Nature 445:851–857. https://doi.org/10.1038/nature05661

Grimm C, Chen C-C, Wahl-Schott C, Biel M (2017) Two-pore channels: catalyzers of endolysosomal transport and function. Front Pharmacol 8:45. https://doi.org/10.3389/fphar.2017.00045

Grossmann S, Mallmann RT, Klugbauer N (2021) Two-pore channels regulate expression of various receptors and their pathway-related proteins in multiple Ways. Cells 10. https://doi.org/10.3390/cells10071807

Grzywa TM, Paskal W, Włodarski PK (2017) Intratumor and Intertumor Heterogeneity in Melanoma. Transl Oncol 10:956–975. https://doi.org/10.1016/j.tranon.2017.09.007

Hachey SJ, Boiko AD (2016) Therapeutic implications of melanoma heterogeneity. Exp Dermatol 25:497–500. https://doi.org/10.1111/exd.13002

Hanbashi A, Alotaibi M, Sobeai HMA, Binobaid L, Alhazzani K, Jin X, Kamli F, Alhoshani A, Parrington J (2023) Loss of two-pore channel 2 function in melanoma-derived tumours reduces tumour growth in vivo but greatly increases tumour-related toxicity in the organism. Cancer Cell Int 23:325. https://doi.org/10.1186/s12935-023-03148-6

Hönigova K, Navratil J, Peltanova B, Polanska HH, Raudenska M, Masarik M (2022) Metabolic tricks of cancer cells. Biochimica et Biophysica Acta (BBA) - Rev Cancer 1877, 188705. https://doi.org/10.1016/j.bbcan.2022.188705

Huang F, Santinon F, Flores González RE, Del Rincón SV (2021) Melanoma Plasticity: Promoter of Metastasis and Resistance to Therapy. Front Oncol 11:756001. https://doi.org/10.3389/fonc.2021.756001

Jin X, Hanbashi AA, Kamli F, Pan X, Goding CR, Parrington J (2024) TPC1 regulates melanoma tumourigenesis via mTORC1 and TFEB. Heliyon 10:e39752. https://doi.org/10.1016/j.heliyon.2024.e39752

Kwon YW, Jo H-S, Bae S, Seo Y, Song P, Song M, Yoon JH (2021) Application of Proteomics in Cancer: Recent Trends and Approaches for Biomarkers Discovery. Front Med (Lausanne) 8. https://doi.org/10.3389/fmed.2021.747333

Lagostena L, Minicozzi V, Meucci M, Gradogna A, Milenkovic S, Palombi F, Ceccarelli M, Filippini A, Carpaneto A (2025) The two-pore channel 2 in human physiology and diseases: functional characterisation and pharmacology. Int J Mol Sci 26. https://doi.org/10.3390/ijms26199708

Latonen L, Afyounian E, Jylhä A, Nättinen J, Aapola U, Annala M, Kivinummi KK, Tammela TTL, Beuerman RW, Uusitalo H, Nykter M, Visakorpi T (2018) Integrative proteomics in prostate cancer uncovers robustness against genomic and transcriptomic aberrations during disease progression. Nat Commun 9:1176. https://doi.org/10.1038/s41467-018-03573-6

Mani DR, Krug K, Zhang B, Satpathy S, Clauser KR, Ding L, Ellis M, Gillette MA, Carr SA (2022) Cancer proteogenomics: current impact and future prospects. Nat Rev Cancer 22:298–313. https://doi.org/10.1038/s41568-022-00446-5

Mookerjee SA, Goncalves RLS, Gerencser AA, Nicholls DG, Brand MD (2015) The contributions of respiration and glycolysis to extracellular acid production. Biochimica et Biophysica Acta (BBA) - Bioenergetics 1847:171–181. https://doi.org/10.1016/j.bbabio.2014.10.005

Moreira A, Heinzerling L, Bhardwaj N, Friedlander P (2021) Current melanoma treatments: where do we stand? Cancers (Basel) 13:221. https://doi.org/10.3390/cancers13020221

Müller M, Gerndt S, Chao Y-K, Zisis T, Nguyen ONP, Gerwien A, Urban N, Müller C, Gegenfurtner FA, Geisslinger F, Ortler C, Chen C-C, Zahler S, Biel M, Schaefer M, Grimm C, Bracher F, Vollmar AM, Bartel K (2021) Gene editing and synthetically accessible inhibitors reveal role for TPC2 in HCC cell proliferation and tumor growth. Cell Chem Biol 28:1119-1131.e27. https://doi.org/10.1016/j.chembiol.2021.01.023

Nadanaciva S, Rana P, Beeson GC, Chen D, Ferrick DA, Beeson CC, Will Y (2012) Assessment of drug-induced mitochondrial dysfunction via altered cellular respiration and acidification measured in a 96-well platform. J Bioenerg Biomembr 44:421–437. https://doi.org/10.1007/s10863-012-9446-z

Netcharoensirisuk P, Abrahamian C, Tang R, Chen C-C, Rosato AS, Beyers W, Chao Y-K, Filippini A, Di Pietro S, Bartel K, Biel M, Vollmar AM, Umehara K, De-Eknamkul W, Grimm C (2021) Flavonoids increase melanin production and reduce proliferation, migration and invasion of melanoma cells by blocking endolysosomal/melanosomal TPC2. Sci Rep 11:8515. https://doi.org/10.1038/s41598-021-88196-6

Ng MF, Simmons JL, Boyle GM (2022) Heterogeneity in melanoma. Cancers. https://doi.org/10.3390/cancers14123030

Nguyen HT, Wiederkehr A, Wollheim CB, Park K-S (2024) Regulation of autophagy by perilysosomal calcium: a new player in β-cell lipotoxicity. Exp Mol Med 56:273–288. https://doi.org/10.1038/s12276-024-01161-x

Nguyen ONP, Grimm C, Schneider LS, Chao Y-K, Atzberger C, Bartel K, Watermann A, Ulrich M, Mayr D, Wahl-Schott C, Biel M, Vollmar AM (2017) Two-pore channel function is crucial for the migration of invasive cancer cells. Cancer Res 77:1427–1438. https://doi.org/10.1158/0008-5472.CAN-16-0852

Ogunbayo OA, Duan J, Xiong J, Wang Q, Feng X, Ma J, Zhu MX, Evans AM (2018) mTORC1 controls lysosomal Ca^{2+} release

through the two-pore channel TPC2. Sci Signal. https://doi.org/10.1126/scisignal.aao5775

Park K, Lim H, Kim J, Hwang Y, Lee YS, Bae SH, Kim H, Kim H, Kang S-W, Kim JY, Lee M-S (2022) Lysosomal Ca2+-mediated TFEB activation modulates mitophagy and functional adaptation of pancreatic β-cells to metabolic stress. Nat Commun 13:1300. https://doi.org/10.1038/s41467-022-28874-9

Ponomarenko EA, Krasnov GS, Kiseleva OI, Kryukova PA, Arzumanian VA, Dolgalev GV, Ilgisonis EV, Lisitsa AV, Poverennaya EV (2023) Workability of mRNA sequencing for predicting protein abundance. Genes. https://doi.org/10.3390/genes14112065

Rambow F, Marine J-C, Goding CR (2019) Melanoma plasticity and phenotypic diversity: therapeutic barriers and opportunities. Genes Dev 33:1295–1318. https://doi.org/10.1101/gad.329771.119

Schmidt CA, Fisher-Wellman KH, Neufer PD (2021) From OCR and ECAR to energy: perspectives on the design and interpretation of bioenergetics studies. J Biol Chem 297:101140. https://doi.org/10.1016/j.jbc.2021.101140

Shuken SR (2023) An introduction to mass spectrometry-based proteomics. J Proteome Res 22:2151–2171. https://doi.org/10.1021/acs.jproteome.2c00838

Sivandzade F, Bhalerao A, Cucullo L (2019) Analysis of the mitochondrial membrane potential using the cationic JC-1 dye as a sensitive fluorescent probe. Bio Protoc 9. https://doi.org/10.21769/BioProtoc.3128

Skelding KA, Barry DL, Theron DZ, Lincz LF (2022) Targeting the two-pore channel 2 in cancer progression and metastasis. Explor Target Antitumor Ther 62–89. https://doi.org/10.37349/etat.2022.00072

Smith PK, Krohn RI, Hermanson GT, Mallia AK, Gartner FH, Provenzano MD, Fujimoto EK, Goeke NM, Olson BJ, Klenk DC (1985) Measurement of protein using bicinchoninic acid. Anal Biochem 150:76–85. https://doi.org/10.1016/0003-2697(85)90442-7

Soura E, Eliades PJ, Shannon K, Stratigos AJ, Tsao H (2016) Hereditary melanoma: update on syndromes and management. J Am Acad Dermatol 74:395–407. https://doi.org/10.1016/j.jaad.2015.08.038

Tooze S, Zoncu R (2015) Control of cellular homeostasis: organelles take the pilot's seat. Mol Biol Cell 26:1009–1010. https://doi.org/10.1091/mbc.E14-12-1589

Toussi A, Mans N, Welborn J, Kiuru M (2020) Germline mutations predisposing to melanoma. J Cutan Pathol 47:606–616. https://doi.org/10.1111/cup.13689

Wang J, Duncan D, Shi Z, Zhang B (2013) WEB-based GEne SeT AnaLysis Toolkit (WebGestalt): update 2013. Nucleic Acids Res 41:W77-83. https://doi.org/10.1093/nar/gkt439

Wang X, Zhang X, Dong X, Samie M, Li X, Cheng X, Goschka A, Shen D, Zhou Y, Harlow J, Zhu MX, Clapham DE, Ren D, Xu H (2012) TPC Proteins Are Phosphoinositide- Activated Sodium-Selective Ion Channels in Endosomes and Lysosomes. Cell 151:372–383. https://doi.org/10.1016/j.cell.2012.08.036

Yuan Y, Jaślan D, Rahman T, Bolsover SR, Arige V, Wagner LE, Abrahamian C, Tang R, Keller M, Hartmann J, Rosato AS, Weiden E-M, Bracher F, Yule DI, Grimm C, Patel S (2022) Segregated cation flux by TPC2 biases Ca2+ signaling through lysosomes. Nat Commun 13:4481. https://doi.org/10.1038/s41467-022-31959-0

Zhang X, Cheng X, Yu L, Yang J, Calvo R, Patnaik S, Hu X, Gao Q, Yang M, Lawas M, Delling M, Marugan J, Ferrer M, Xu H (2016) MCOLN1 is a ROS sensor in lysosomes that regulates autophagy. Nat Commun 7:12109. https://doi.org/10.1038/ncomms12109

Zhu MX, Ma J, Parrington J, Calcraft PJ, Galione A, Evans AM (2010) Calcium signaling via two-pore channels: local or global, that is the question. Am J Physiol Cell Physiol 298:C430–C441. https://doi.org/10.1152/ajpcell.00475.2009

Zhu N, Yang R, Wang X, Yuan L, Li X, Wei F, Zhang L (2023) The hippo signaling pathway: from multiple signals to the hallmarks of cancers. Acta Biochim Biophys Sin (Shanghai) 55:904–913. https://doi.org/10.3724/abbs.2023035